The EMBO Journal Vol.16 No.22 pp.6615–6625, 1997

Kv2.1/Kv9.3, a novel ATP-dependent delayed-rectifier K^+ channel in oxygen-sensitive pulmonary artery myocytes

Amanda J.Patel, Michel Lazdunski[1] and Eric Honoré

Institut de Pharmacologie Moléculaire et Cellulaire, CNRS, 660 route des Lucioles, Sophia Antipolis, 06560 Valbonne, France

[1]Corresponding author
e-mail: ipmc@unice.fr

The molecular structure of oxygen-sensitive delayed-rectifier K^+ channels which are involved in hypoxic pulmonary artery (PA) vasoconstriction has yet to be elucidated. To address this problem, we identified the *Shab* K^+ channel Kv2.1 and a novel *Shab*-like subunit Kv9.3, in rat PA myocytes. Kv9.3 encodes an electrically silent subunit which associates with Kv2.1 and modulates its biophysical properties. The Kv2.1/9.3 heteromultimer, unlike Kv2.1, opens in the voltage range of the resting membrane potential of PA myocytes. Moreover, we demonstrate that the activity of Kv2.1/Kv9.3 is tightly controlled by internal ATP and is reversibly inhibited by hypoxia. In conclusion, we propose that metabolic regulation of the Kv2.1/Kv9.3 heteromultimer may play an important role in hypoxic PA vasoconstriction and in the possible development of PA hypertension.

Keywords: dex-fenfluramine/hypoxia/oxygen-sensitivity/pulmonary hypertension/vasoconstriction

Introduction

Oxygen is an essential requirement for cell survival. However, the organism has the ability to adapt rapidly to hypoxia. Ion channels, in particular K^+ channels, play a key role in adaptive hypoxic mechanisms and are thought to be involved in the sensing of oxygen (Lopez-Barneo, 1994, 1996; Kozlowski, 1995; Weir and Archer, 1995; Lopez-Barneo *et al.*, 1997). One such adaptation is the hypoxia-induced vasoconstriction of resistance pulmonary artery (PA) smooth muscle which leads to a redistribution of the non-oxygenated blood towards better ventilated regions of the lung (for review, see Kozlowski, 1995; Weir and Archer, 1995). In the fetus, hypoxic pulmonary vasoconstriction (HPV) diverts blood through the ductus arteriosus and is essential for fetal survival. Although HPV fulfils an essential physiological function, it also contributes to the development of pulmonary hypertension in patients with chronic obstructive lung diseases (e.g. chronic bronchitis, emphysema) and people living at high altitudes (Barnes and Liu, 1995; Weir and Archer, 1995). It has been demonstrated that hypoxic vasoconstriction of resistance PA smooth muscle cells is mainly mediated by the closing of voltage-dependent K^+ channels leading to cell depolarization, calcium influx and myocyte contraction (Post *et al.*, 1992; Archer *et al.*, 1993; Yuan *et al.*, 1993a; Cornfield *et al.*, 1994; Osipenko *et al.*, 1997). Chronic hypoxia has also been associated with reduced delayed-rectifier K^+ current in rat pulmonary artery smooth muscle cells (Smirnov *et al.*, 1994). Recently, a novel oxygen-sensitive non-inactivating K^+ current active at resting membrane potential ($I_{K(N)}$) has been described in rabbit PA myocytes (Evans *et al.*, 1996; Osipenko *et al.*, 1997).

The molecular identity of these oxygen-sensitive K^+ channels and the nature of the oxygen sensor(s) remain unknown. The present work reports the molecular cloning, characterization and regulation by hypoxia of a novel voltage- and ATP-dependent K^+ channel subunit called Kv9.3, isolated from rat PA smooth muscle cells. The molecular identification of Kv9.3 could be of tremendous importance in the understanding of pulmonary hypertension and in the design of novel therapeutic strategies.

Results

Delayed-rectifier K^+ channels in rat pulmonary artery myocytes

In order to record selectively the activity of voltage-dependent K^+ channels in PA smooth muscle, cells were voltage-clamped in the whole-cell configuration in the absence of external and internal calcium (10 mM EGTA) and in the presence of 5 mM internal ATP to avoid contamination with both large conductance calcium-dependent K^+ channels and K_{ATP} channels (Yuan *et al.*, 1996). Figure 1A and B compare the I–V relationships of the currents recorded in freshly dissociated and cultured PA cells. The characteristics of the outward currents observed in freshly dissociated cells were identical to those in primary (I) culture. However, when the cells were trypsinized and plated in secondary (II) culture, the outward K^+ currents were absent (Figure 1B). Similar data were obtained with passages III to VIII (not shown). During maintained depolarization, the outward K^+ current declined with an exponential time course ($\tau = 271 \pm 48$ ms at + 50 mV, $n = 18$). Steady-state activation and inactivation parameters of currents recorded in primary cultured PA cells are presented in Figure 1C. The activation voltage threshold was –50 mV, a value close to the resting membrane potential (–54 ± 4 mV, $n = 6$). About 15% of the channels failed to inactivate at +20 mV (Figure 1C). The activation and inactivation steady-state curves overlapped, revealing a window K^+ current. The pharmacological properties of the PA myocyte K^+ channels are illustrated in Figure 1D. Charybdotoxin (CTX; 20 nM), dendrotoxin (DTX; 200 nM) and mast cell degranulating peptide (MCD; 300 nM), potent blockers of both Kv1.2 and Kv1.3, inhibited the outward current by ~20%, with the effects of DTX and CTX being non-additive. In agreement with previous reports (Post *et al.*, 1995; Yuan,

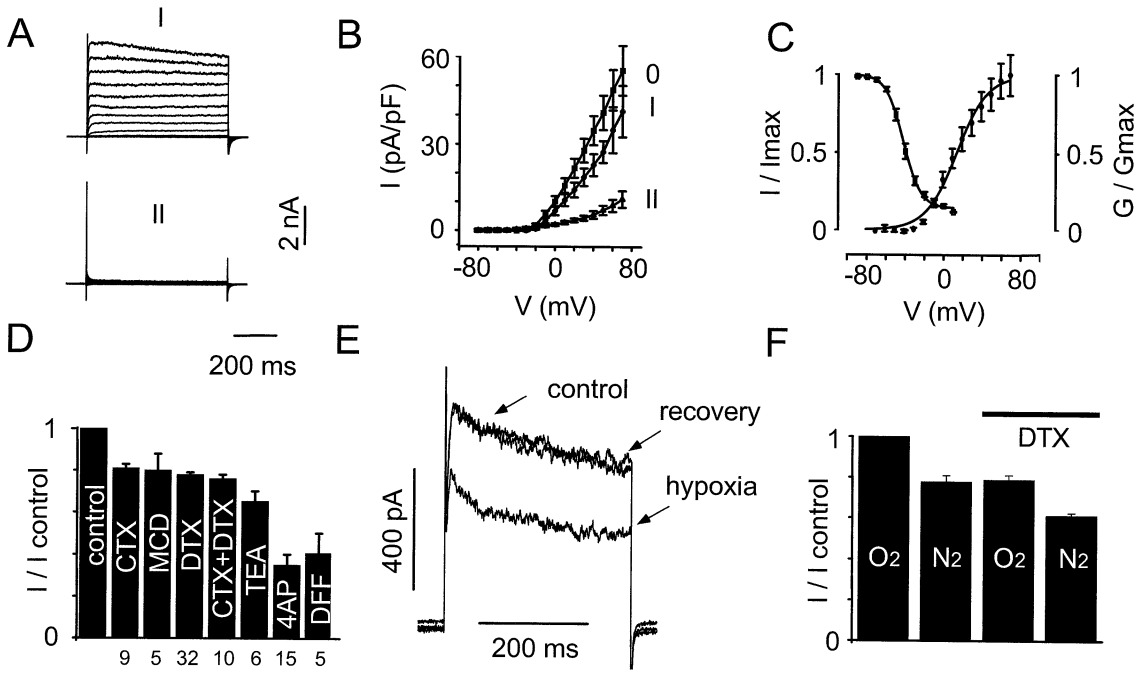

Fig. 1. Delayed-rectifier K^+ channels in rat resistance pulmonary artery myocytes. (**A**) K^+ channel currents in PA myocytes maintained either in primary (I) or secondary (II) culture (n = 7). The holding potential was –80 mV and the cells were depolarized from –60 mV to +40 mV by 10 mV increments. (**B**) *I–V* curves of freshly dissociated, primary and secondary cultured PA resistance myocytes. (**C**) Steady-state activation (V0.5: +3 mV, k: 17.6 mV) and inactivation (60 s prepulse duration) curves (V0.5: –42 mV, k: 9.1 mV) of PA myocytes K^+ channels (n = 7). (**D**) Pharmacology of K^+ channels in PA myocytes. The effects of 20 nM charybdotoxin (CTX), 300 nM mast cell degranulating factor (MCD), 200 nM dendrotoxin (DTX), 3 mM tetraethylammonium (TEA), 1 mM 4-aminopyridine (4-AP) and 1 mM dex-fenfluramine (DFF) are indicated. Numbers of cells are indicated. (**E**) Reversible hypoxic inhibition of outward K^+ current in PA myocytes. The holding potential was –80 mV and the test pulse +30 mV. (**F**) Hypoxic inhibition of outward K^+ current elicited by a test pulse at +30 mV in myocytes either in the absence (N_2) or the presence (N_2/DTX) of 200 nM DTX (n = 6).

1995; Archer *et al.*, 1996), we observed that outward K^+ currents in PA smooth muscle cells are relatively resistant to tetraethylammonium (TEA) but sensitive to 4-aminopyridine (4-AP). Finally, the appetite-suppressant drug dex-fenfluramine (DFF) which has been shown to induce PA vasoconstriction (Weir *et al.*, 1996) inhibited the outward K^+ current by 60% at a concentration of 1 mM. The sensitivity of resistance PA myocytes K^+ channels to hypoxia is illustrated in Figure 1E. The hypoxic inhibition of K^+ currents in the presence and in the absence of 200 nM DTX was compared (Figure 1F). Hypoxic inhibitions (25 ± 4% and 17 ± 2% in control and in the presence of DTX, respectively) were not statistically different (P <0.05) between the two experimental conditions.

Cloning of delayed-rectifier K^+ channel subunits from pulmonary artery myocytes

A degenerate PCR-based strategy was used to identify at the molecular level, potential PA oxygen-sensitive K^+ channels. Our degenerate primers were designed in two highly conserved regions in *Shaker*, *Shab*, *Shaw* and *Shal* family members, namely a region upstream of S1 (the first transmembrane domain) and a region in the pore (the H5 domain) (Figure 2A). Following this procedure, Kv1.2, Kv1.3, Kv2.1 and a novel K^+ channel, Kv9.3 were identified in PA myocytes (Figures 2A and 3A). As negative controls, specific oligonucleotides for Kv1.5 (Figure 3A) and Kv2.2 (data not shown) were used to show the absence of these transcripts in PA cell templates (conduit and resistance) although a strong signal was always observed within the brain. The amino acid sequence of Kv9.3 (through S6) is aligned with that of Kv2.1 in Figure 2A. Kv9.3 bears all the classical hallmarks of a voltage-gated K^+ channel with six potential transmembrane domains (S1–S6), S4 containing five positively-charged amino acids and a conserved pore region, H5, between S5 and S6. Alignment of Kv9.3 with other voltage-gated K^+ channels shows that it is most homologous to *Shab* family members, sharing the highest identity with Kv9.2 at 52.4%. The phylogenetic tree presented in Figure 2B demonstrates that Kv9.3 belongs to a novel family of electrically silent K^+ channel subunits including Kv5, Kv6, Kv8 and Kv9 (Salinas *et al.*, 1997b) members. Northern blot analysis of various rat tissues reveals a single transcript for Kv9.3 at 3.2 kb, the most abundant of which is in lung (Figure 3B). In order to define the spatial expression of Kv1.2, Kv1.3, Kv2.1 and Kv9.3, RT–PCR was performed with RNA from different tissues including lung, brain, conduit artery and resistance artery cells (primary and secondary cultures) (Figure 3A). All the transcripts were found in the lung and brain. A differential pattern of expression is observed between conduit and resistance PA cells. Kv1.2 and Kv2.1 are expressed at higher levels in conduit artery. By contrast, Kv1.3 is only expressed in resistance artery whereas, Kv9.3 was similarly expressed in both tissues. Furthermore, only Kv9.3 was detected in cells maintained in secondary culture.

Functional expression of Kv9.3 in COS cells and Xenopus oocytes

The cDNA encoding Kv9.3 was cloned into the expression vector pCI and either transfected in COS-M6 cells or

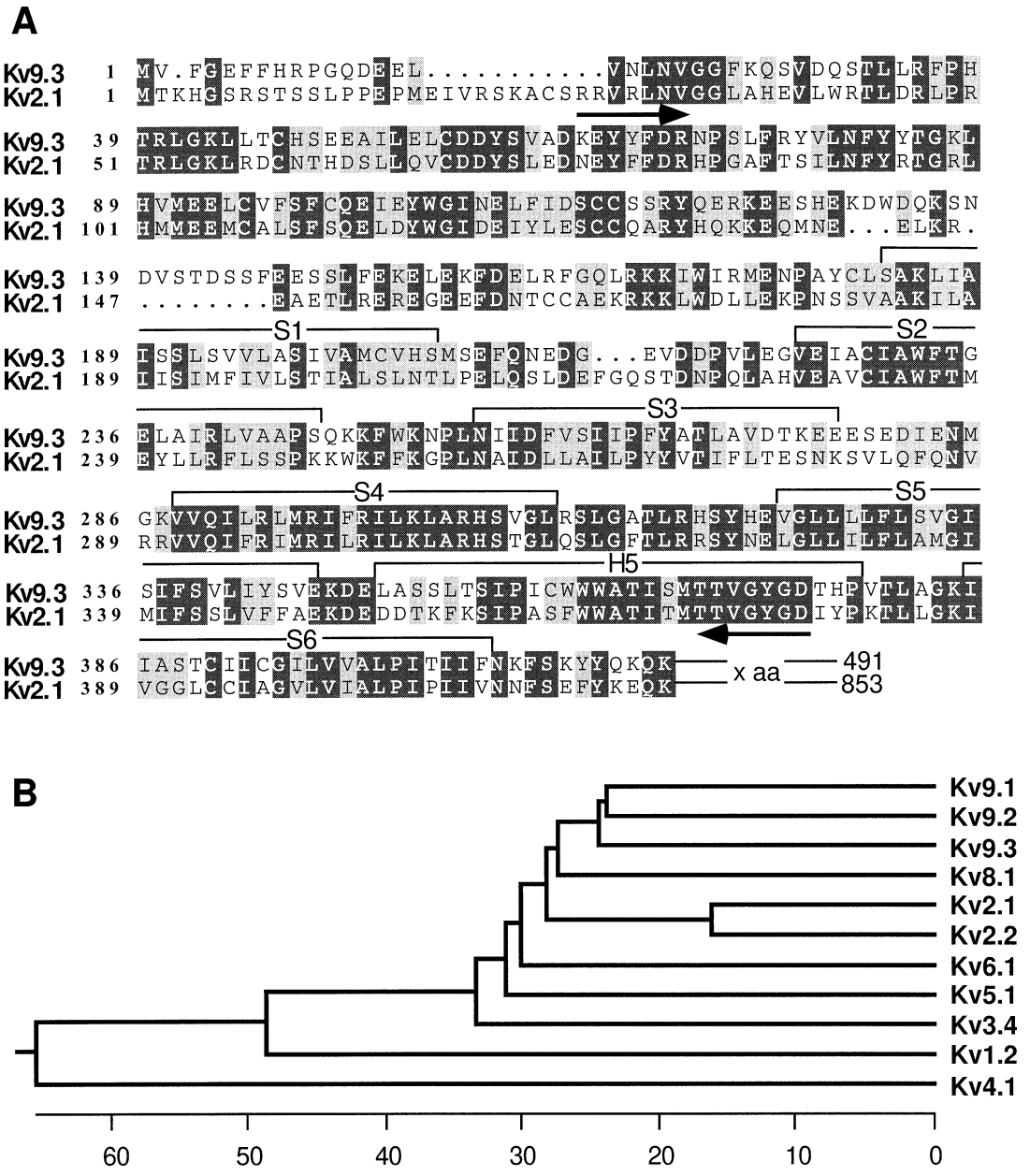

Fig. 2. Sequence comparison, expression and phylogeny of Kv9.3. (**A**) Alignment of Kv9.3 and Kv2.1 amino acid sequences through S6. Identical and conserved residues are boxed in black and grey, respectively. Dots indicate gaps introduced for better alignment. Relative positions of putative transmembrane domains (S1–S6) and the pore (H5) are also indicated. Arrows indicate the positions of the degenerate primers. Regions beyond S6 were not aligned since there was little conservation and are indicated by x aa. (**B**) Phylogenetic tree demonstrating the ancestral relationships between the voltage-dependent K^+ channels indicated (Clustal method). The scale beneath the tree measures the distance between sequences. The sequence of Kv9.3 has been deposited in the Genbank/EMBL database under the accession No. AF 029056.

injected into *Xenopus* oocyte nuclei (Figure 4). pCI–Kv9.3-expressing cells did not express any exogenous channel activity (Figure 4B). However, when pCI–Kv9.3 was co-expressed with pCI–Kv2.1 (also identified in PA cells), we observed an important modification of the Kv2.1 channel properties recorded in a physiological K^+ gradient (Figure 4A and B). The activation threshold was shifted towards negative values (–50 mV) and the amplitude of the currents were enhanced in the presence of Kv9.3 (Figure 4B). Control oocytes had a RMP of –34 ± 3 mV (n = 10) and Kv2.1 and Kv2.1/Kv9.3-expressing oocytes displayed RMPs of –53 ± 4 mV (n = 8) and –58 ± 4 mV (n = 9), respectively. The RMPs of control, Kv9.3-, Kv2.1- and Kv2.1/Kv9.3-expressing COS cells were 3.9 ± 5 mV (n = 10), 6.3 ± 3.6 mV (n = 7), –30.7 ± 1.3 mV (n = 10) and –50.6 ± 0.9 mV (n = 15), respectively. Tail current analysis was used to estimate the reversal potentials and to construct steady-state activation curves. The reversal potential of the tail currents was identical for Kv2.1 (–84 ± 3 mV, n = 7) and Kv2.1/Kv9.3 (–86 ± 4 mV, n = 8). Both steady-state activation and inactivation curves of Kv2.1 were displaced towards more negative values by ~20 mV in the presence of Kv9.3 (Figure 4C). Besides the alteration of the steady-state activation and inactivation parameters, Kv9.3 also had an important effect on the activation and deactivation kinetics

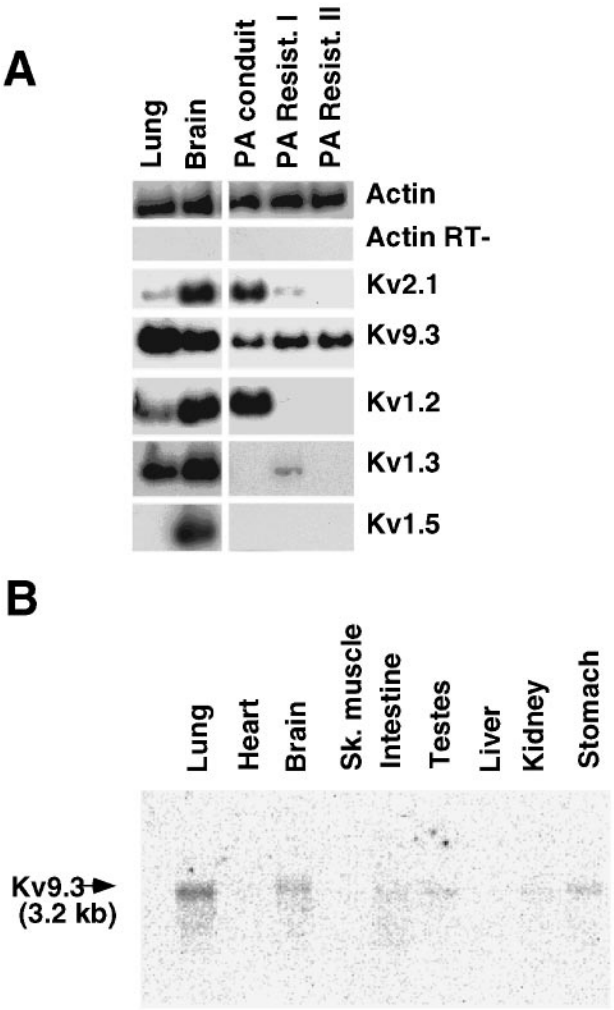

Fig. 3. Spatial expression of pulmonary artery K^+ channel subunits. (**A**) RT–PCR was performed on RNA from the tissues indicated (see top) with primers against actin or the K^+ channel subunits shown (see side). (**B**) The expression of Kv9.3 was analysed by Northern blot in adult rat tissues. Each lane represents 15 μg of total RNA. The size of the messenger is indicated.

(Figure 4A and D–F). Kv9.3 speeded up the activation and slowed down the deactivation of Kv2.1. To verify that the effects of Kv9.3 were specific for Kv2.1, pCI–Kv9.3 was co-injected with either pCI–Kv1.2 or pCI–Kv1.3 (also identified in PA cells) into *Xenopus* oocytes. No effect was found on the biophysical properties of both Kv1.2 and Kv1.3 ($n = 6$; data not shown).

Single-channel properties of Kv2.1/Kv9.3

Examination of the single-channel properties of Kv2.1 and Kv2.1/Kv9.3 revealed that Kv9.3 alters the single-channel conductance of Kv2.1 (Figure 5A and B). In the cell-attached mode and in inside-out patch configuration, Kv2.1 has a single-channel conductance of 8.5 and 6.2 pS, respectively (physiological K^+ gradient). However, when co-expressed with Kv9.3, the single-channel conductance was 14.5 pS and 12.7 pS (cell-attached and inside-out configurations). In some patches, from cells co-expressing Kv9.3 and Kv2.1, both single-channel conductances (8.5 and 14.5 pS) were observed. No intermediate single-channel conductance was observed in patches from Kv2.1/Kv9.3-expressing cells. Figure 5C shows single-channel recordings from a cell-attached patch at different potentials and demonstrates that the open state probability of Kv2.1/Kv9.3 was dependent on the voltage as expected from the measured whole-cell currents (Figure 4). The *I–V* curve measured using a voltage ramp protocol shows that the activation threshold was –50 mV and that a mild inward rectification was observed at positive potentials (Figure 5D).

Kv2.1/Kv9.3 is regulated by internal ATP

The activity of both Kv2.1 and Kv2.1/Kv9.3 in excised inside-out patches was sensitive to the presence of internal ATP. Figure 6A compares the effects of various ATP concentration conditions and the effects of ATPγs and AMP–PNP on Kv2.1/Kv9.3 channel activity. When ATP concentration was lowered from 5 mM to 1 mM, channel activity was reduced by 55%. ATP-free solution or substitution of ATP by AMP–PNP both produced a decrease of ~80% in Kv2.1/Kv9.3 channel activity. However, when ATP was substituted by ATPγs, channel activity was only reduced by 50%. Similar data were obtained with Kv2.1 alone (not shown). Channel activity was insensitive to internal ADP (Figure 6A). The possible implication of internal ATP in channel phosphorylation was then studied using alkaline phosphatase ($n = 5$). Figure 6B and C show that channel activity observed in the presence of 5 mM internal ATP could be reversibly inhibited by alkaline phosphatase.

Pharmacological properties of the Kv2.1/Kv9.3 channel

Figure 7 shows that the pharmacological properties of Kv2.1 were altered when co-expressed with Kv9.3 in *Xenopus* oocytes. Both the sensitivity to TEA and 4-AP were decreased by 3- and 10- fold, respectively (Figure 7A and B). Figure 7C shows the effect of 4-AP on the *I–V* curve of Kv2.1/Kv9.3 recorded in a K^+-rich solution. This protocol allows the amplification of K^+-currents at negative potentials, in the range of the activation threshold and demonstrates that 4-AP shifts the mid-point activation potential of Kv2.1/Kv9.3. Kv2.1 and Kv2.1/Kv9.3 were insensitive to 50 nM CTX and 200 nM DTX ($n = 3$, not shown). Figure 7D and E shows that DFF is a potent blocker of Kv2.1 and Kv2.1/Kv9.3. Both channels displayed the same sensitivity to DFF (IC_{50} 300 μM). The effect of increasing concentrations of DFF on the Kv2.1/Kv9.3 *I–V* curve recorded in COS cells is shown in Figure 7E.

Co-immunoprecipitation of Kv9.3 with Kv2.1

The previous data suggested that Kv9.3 may associate with Kv2.1 to form a heteromultimer whose biophysical and pharmacological properties were different from the Kv2.1 homomultimer. In order to demonstrate a direct interaction between Kv2.1 and Kv9.3, immunoprecipitation experiments were performed with metabolically labelled *Xenopus* oocytes injected with pCI–Kv9.3, pCI–Kv2.1, or both. Figure 8 shows that anti-Kv2.1 immunoprecipitates three major species (see inset) in Kv2.1-expressing oocytes in the range of 110 kDa, which probably correspond to phosphorylated forms of Kv2.1 as has been previously reported (Shi *et al.*, 1994). No

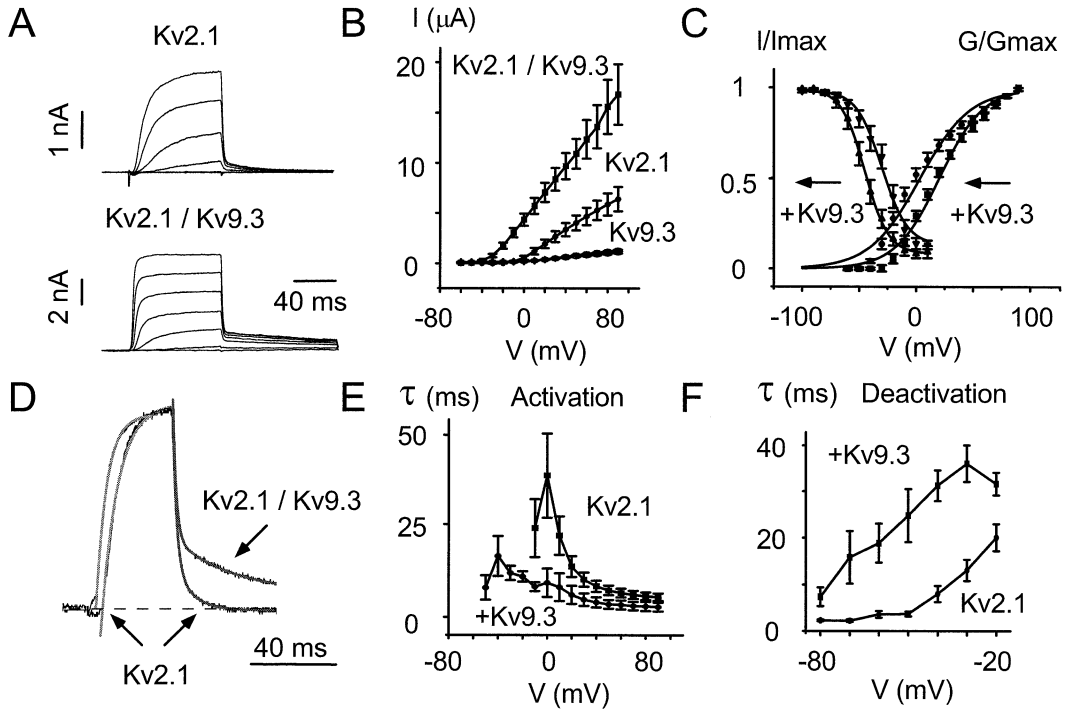

Fig. 4. Functional expression of Kv9.3 in *Xenopus* oocytes and COS cells. (**A**) Typical recordings of Kv2.1 (top) and Kv2.1/Kv9.3 (bottom) in transfected COS cells. The holding potential was –60 mV and cells were depolarized by 10 mV increments to 0 mV in a physiological K^+ gradient. (**B**) *I–V* curves of K^+ currents recorded in injected oocytes (n = 10). (**C**) Steady-state activation (for Kv2.1, V0.5: 20.4 mV, k: 19.6 mV and for Kv2.1/Kv9.3, V0.5: 3.2 mV, k: 21.8 mV) and inactivation (60 s prepulse duration) curves (for Kv2.1/Kv9.3, V0.5: –44.9 mV, k: 10.4 mV and for Kv2.1, V0.5: –29.8 mV, k: 11.1 mV) of Kv2.1 and Kv2.1/Kv9.3 (n = 7). (**D**) Scaled current traces for Kv2.1 and Kv2.1/Kv9.3. Currents were elicited by test voltage pulses to +10 mV from a holding potential of –80 mV. Activations were fitted with power functions of the first order $\{I\times[1-\exp(-(t-K)/\tau)]+C\}$ and deactivations were fitted with the sum of two exponentials. Activation time constants were 7 and 4.9 ms for Kv2.1 and Kv2.1/Kv9.3, respectively. Fast deactivation time constants were 1.8 ms and 1.5 ms and slow deactivation time constants were 8.5 and 28 ms for Kv2.1 and Kv2.1/Kv9.3, respectively. (**E**) Relationships between activation time constants and test pulse voltages for Kv2.1 and Kv2.1/Kv9.3 (n = 7). (**F**) Relationship between the slow deactivation time constant and test pulse voltages for Kv2.1 and Kv2.1/Kv9.3 (n = 7).

expression of immunoreactive Kv2.1 protein was detected in control oocytes (lane 1). However, when Kv2.1 was co-expressed with Kv9.3, an additional band of ~56 kDa was detected. This band migrates in the same size range as the *in vitro*-translated Kv9.3 (data not shown) and is absent in control oocytes. Protein A–Sepharose alone did not precipitate either Kv2.1 or Kv9.3 (data not shown).

Effects of hypoxia on Kv2.1 and Kv2.1/Kv9.3

In a subset of transfected COS cells, Kv2.1 (21% of the cells, n = 14) and Kv2.1/Kv9.3 (56% of the cells, n = 39) were reversibly inhibited by hypoxia (effect >10% inhibition). Figure 9 shows the reversible hypoxic inhibition of Kv2.1 and Kv2.1/Kv9.3. The mean hypoxic inhibitions of the responsive cells were 34 ± 5.5% and 28 ± 2.5% for Kv2.1 and Kv2.1/Kv9.3, respectively. Kv1.2 and Kv1.3 did not display any hypoxic sensitivity in COS cells (n = 11; data not shown). The I–V curves illustrated in Figure 9D show that the effects of hypoxia were independent of the voltage.

Discussion

Molecular identification of K^+ channel subunits in rat PA smooth muscle cells

The aim of the present work was to identify the oxygen-sensitive voltage-dependent delayed-rectifier K^+ channels in rat pulmonary artery smooth muscle cells. Using a PCR approach, we isolated two *Shaker* subunits Kv1.2 and Kv1.3 (Baumann *et al.*, 1988; Stühmer *et al.*, 1989; Beckh and Pongs, 1990; Pongs, 1992), one *Shab* subunit Kv2.1 (Frech *et al.*, 1989) and a novel *Shab*-related subunit called Kv9.3. The presence of Kv1.2 and Kv1.3 was confirmed at the pharmacological level in PA cells using CTX (blocker of both Kv1.2 and Kv1.3) and DTX and MCD peptide (blockers of Kv1.2). This analysis revealed that the DTX-sensitive channels underly ~20% of the total K^+ channel current in PA cells and do not play a significant role in the oxygen-sensitive K^+ channel complexes. Previous reports have clearly demonstrated that hypoxic pulmonary artery vasoconstriction is unaffected by TEA and CTX, blockers of both Kv1.2 and Kv1.3 (Post *et al.*, 1995; Yuan, 1995; Archer *et al.*, 1996). Therefore, these and our present data strongly suggest that Kv1.2 and Kv1.3 do not play a major role as oxygen-sensitive K^+ channels in PA myocytes. Delayed-rectifier K^+ channels $I_{K(V)}$ and $I_{K(A)}$ have been identified in PA myocytes (Post *et al.*, 1992; Yuan *et al.*, 1993b; Smirnov *et al.*, 1994; Yuan, 1995; Archer, 1996; Archer *et al.*, 1996). $I_{K(V)}$ activates and inactivates rather slowly, whereas $I_{K(A)}$ is a transient current. Kv1.3 shares similarities with the native $I_{K(A)}$ channel recorded in PA myocytes (Honoré *et al.*, 1992), while the existence of both Kv2.1 and Kv1.2 may account for $I_{K(V)}$. Since Kv2.1, Kv1.2 and Kv1.3 are all sensitive to 4-AP, they may account for the 4-AP-sensitive component of PA myocytes.

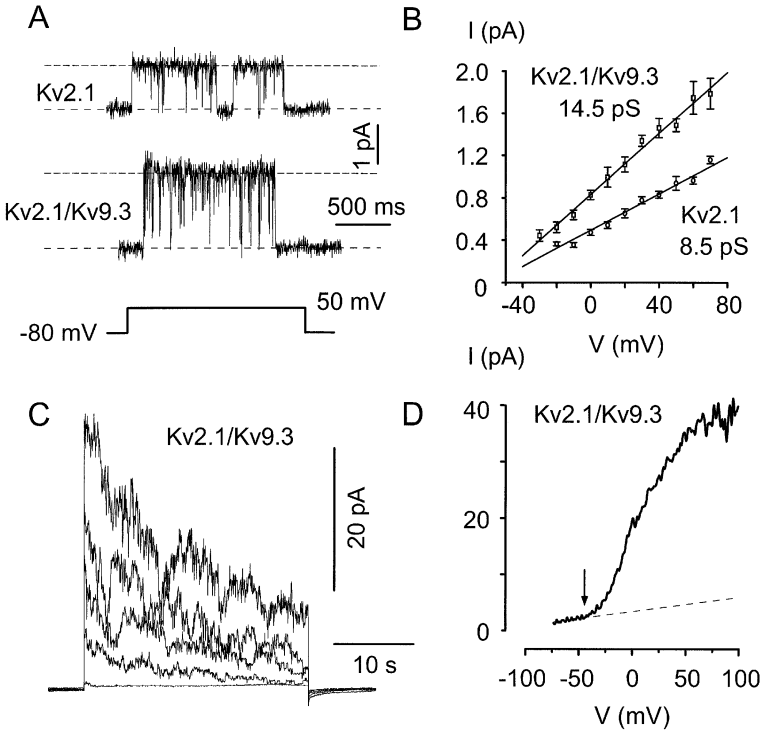

Fig. 5. Single-channel conductance of Kv2.1 and Kv2.1/Kv9.3. (**A**) Typical current traces of Kv2.1 channel (top) and Kv2.1/Kv9.3 channel (bottom) recorded at +50 mV in cell-attached patches under a physiological K^+ gradient from transfected COS cells. (**B**) *I–V* curves of Kv2.1 (n = 8) and Kv2.1/Kv9.3 (n = 8). (**C**) Single-channel recordings in a cell-attached patch at different membrane potentials showing that the open state probability depends on the voltage. The patch was held at –80 mV and depolarizing voltage steps were applied to –50, –20, +10, +40 and +70 mV. (**D**) *I–V* curve recorded during a voltage ramp from –80 mV to +100 mV [same patch as (C)]. The duration of the voltage ramp was 350 ms. The activation voltage threshold is indicated by an arrow.

Kv9.3 associates with Kv2.1 and alters its biophysical and pharmacological properties

The novel *Shab*-related subunit, Kv9.3 encodes an electrically silent K^+ channel subunit when expressed in *Xenopus* oocytes and COS cells. However, this silent channel causes important alterations in the biophysical properties of the *Shab* channel Kv2.1. In particular, Kv9.3 consistently increased Kv2.1 channel current amplitude and shifted steady-state activation towards negative values (–60 to –50 mV). Furthermore, we observed that Kv2.1/Kv9.3 expression induced a shift in the resting membrane potential of both *Xenopus* oocytes and transfected COS cells (from +4 to –51 mV). The ability of Kv9.3 to 'drag' the Kv2.1 activation voltage threshold into the range of PA myocytes RMP suggests that the Kv2.1/Kv9.3 channel complex may contribute to the setting of the RMP (–54 ± 4 mV) and, consequently, in the setting of the resting pulmonary arterial pressure. Kv9.3 also speeded up Kv2.1 activation and dramatically slowed down deactivation. The slowing down of the deactivation was particularly evident in the voltage range corresponding to the resting membrane potential (RMP) of PA myocytes (–50 mV). The steep voltage-dependency of Kv2.1/Kv9.3 suggests that besides its possible role in the establishment of the RMP, this channel may also play an essential role in the control of the PA myocyte action potential duration. Recently, a novel K^+ current $I_{K(N)}$ that is active at resting membrane potential, has been described in rabbit PA smooth muscle cells (Evans *et al.*, 1996; Osipenko *et al.*, 1997). This current is voltage-gated with an activation threshold between –80 and –65 mV in K^+-rich solution. $I_{K(N)}$ was recorded at all levels of the pulmonary artery tree and was found to be blocked by 4-AP with 50% inhibition at 10 mM (Evans *et al.*, 1996). Most importantly, the close similarity between the biophysical and pharmacological characteristics of $I_{K(N)}$ and the $I_{Kv2.1/Kv9.3}$ suggests that the channels underlying these currents may be one and the same.

The alterations in the macroscopic properties of Kv2.1 channel current were confirmed at the single-channel level. Kv9.3 increased the single-channel conductance of Kv2.1, from 8.5 to 14.5 pS. At the pharmacological level, the sensitivity to both 4-AP and TEA were reduced when Kv2.1 was co-expressed with Kv9.3. The alterations in the biophysical and pharmacological properties of Kv2.1 by Kv9.3 suggest that these two subunits associate to form a heteromultimer whose properties are different from that of the Kv2.1 homomultimer. Indeed, immunoprecipitation experiments demonstrated a direct interaction between Kv2.1 and Kv9.3.

Kv9.3 belongs to a novel family of electrically silent K^+ channels and is the first to be identified in vascular smooth muscle. Other members of this new family have previously been identified in brain (Drewe *et al.*, 1992; Hugnot *et al.*, 1996; Salinas *et al.*, 1997a). These channel subunits do not express a K^+ channel current by themselves, but induce profound changes in the properties of the *Shab* channels Kv2.1 and Kv2.2 (Hugnot *et al.*, 1996; Post *et al.*, 1996; Salinas *et al.*, 1997a). Most interestingly, these silent subunits have the ability to create a diverse range of effects, since Kv8.1 acts as a dominant inhibitory

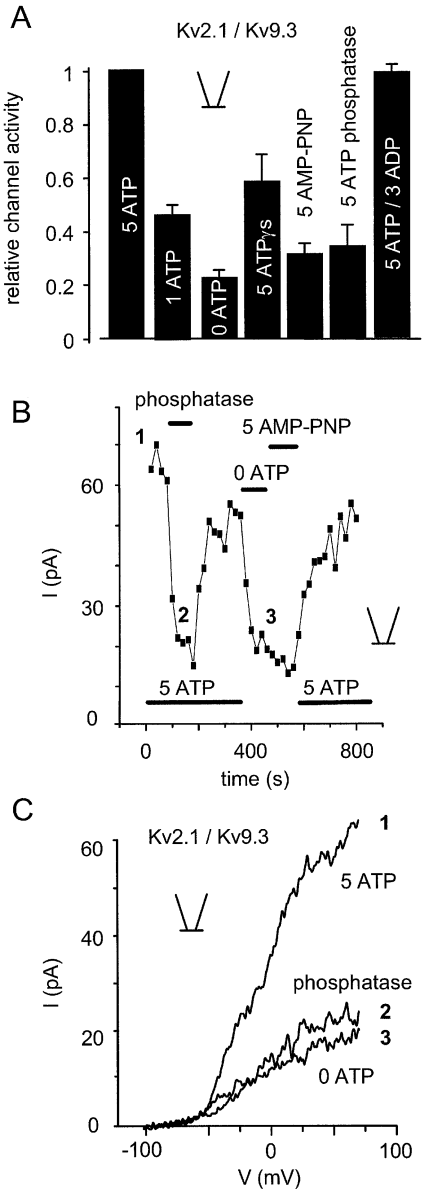

Fig. 6. Kv2.1 and Kv2.1/Kv9.3 are regulated by internal ATP. (**A**) Effects of nucleotides (as indicated) on Kv2.1/Kv9.3 channel activity in independent inside out patches from transfected COS cells in a physiological K^+ gradient. 100 IU/ml alkaline phosphatase was used in these experiments. The number of cells varies from 5 to 11 between the different experimental conditions. (**B**) Reversible effects of alkaline phosphatase (50 IU/ml), free-ATP and 5 mM AMP–PNP on Kv2.1/Kv9.3 channel activity in an inside-out patch (n = 5). (**C**) Corresponding *I–V* curves are represented (as indicated by numbers). The patch was held at –100 mV and depolarized to +80 mV with a voltage ramp of 350 ms in duration.

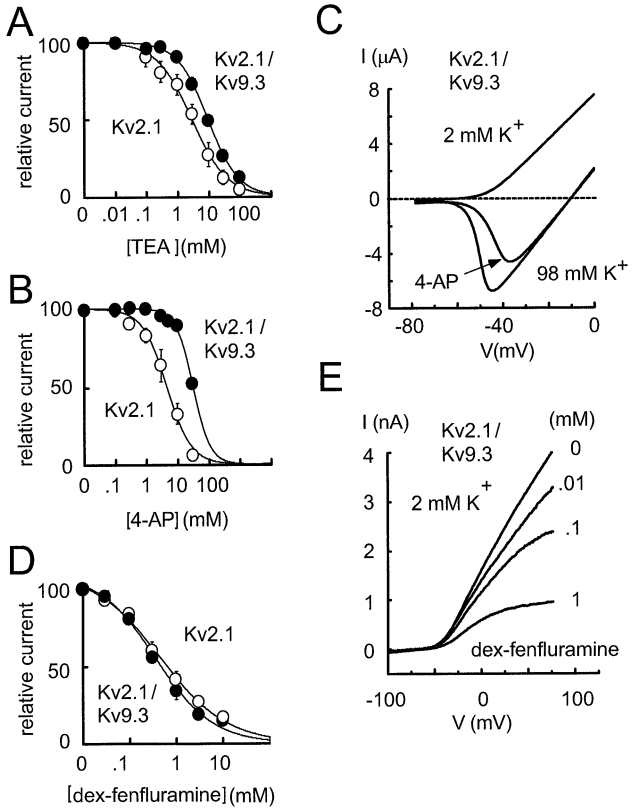

Fig. 7. Pharmacology of Kv2.1 and Kv2.1/Kv9.3. (**A**) Tetraethylammonium concentration–effect curves of Kv2.1 (IC_{50}: 2.9 mM, n = 7) and Kv2.1/Kv9.3 (IC_{50}: 9.5 mM, n = 6) expressed in *Xenopus* oocytes. Currents were measured during a pulse at 10 mV from a holding potential of –60 mV. (**B**) 4-aminopyridine concentration–effect curves of Kv2.1 (IC_{50}: 4.5 mM, n = 6) and Kv2.1/Kv9.3 (IC_{50}: 31.6 mM, n = 6) expressed in *Xenopus* oocytes. Currents were measured during a pulse at 10 mV from a holding potential of –60 mV. (**C**) Effects of 10 mM 4-AP on the *I–V* curve of Kv2.1/Kv9.3 expressed in *Xenopus* oocytes and recorded in a K^+-rich solution (98 mM). (**D**) Dex-fenfluramine concentration–effect curves of Kv2.1 (IC_{50}: 446 μM, n = 5) and Kv2.1/Kv9.3 (IC_{50}: 354 μM, n = 5) expressed in *Xenopus* oocytes. Currents were measured during a pulse at 10 mV from a holding potential of –60 mV. (**E**) Effects of increasing concentrations of dex-fenfluramine (as indicated) on the Kv2.1/Kv9.3 *I–V* curves recorded in transfected COS cells. The holding potential was –80 mV and the cell was depolarized with a voltage ramp to +100 mV. The duration of the ramp was 350 ms.

subunit (Hugnot *et al.*, 1996) while Kv9.3 behaves as a stimulatory one (the present report).

The Kv2.1/Kv9.3 complex is modulated by internal ATP

Our electrophysiological data demonstrate that internal ATP plays an essential role in the control of Kv2.1 and Kv2.1/Kv9.3 channel activity. In inside-out patches, removal of ATP reversibly inhibits channel activity. This is in contrast to what is observed for K_{ATP} channels which are blocked by the presence of ATP (for review, see Quast and Cook, 1989). Similar inhibition was obtained when ATP was substituted with the poorly hydrolysable ATP analogue AMP–PNP. Moreover, the inhibition induced by alkaline phosphatase and the partial activation by ATPγs favour the hypothesis of an ATP regulation via a phosphorylation mechanism. The effects of ATP-free solution and alkaline phosphatase could be obtained repetitively with complete recovery after washout in the absence of any added kinase. This indicates that an endogenous kinase may be closely associated with the channel or may even be a structural part of the channel structure itself. Both Kv2.1 and Kv9.3 contain numerous putative phosphorylation sites including PKA, PKC and calcium–calmodulin kinase sites. Additionally, Kv9.3 contains a putative phosphorylation site for tyrosine kinase. Further studies will be required to identify the exact nature of the modulation and the phosphorylation sites involved in the regulation of the Kv2.1/Kv9.3 complex by internal ATP.

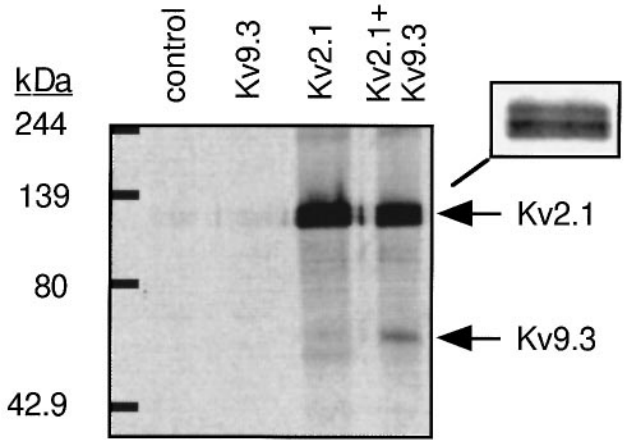

Fig. 8. Immunoprecipitation of Kv2.1 and Kv9.3. Immunoprecipitation of Kv2.1 and Kv9.3 from metabolically labelled *Xenopus* oocytes, injected either with empty expression vector pCI (control) or with pCI–Kv9.3, pCI–Kv2.1 or both. The inset shows a magnification and a lower exposure of the Kv2.1 triplet. Arrows indicate Kv2.1 or Kv9.3.

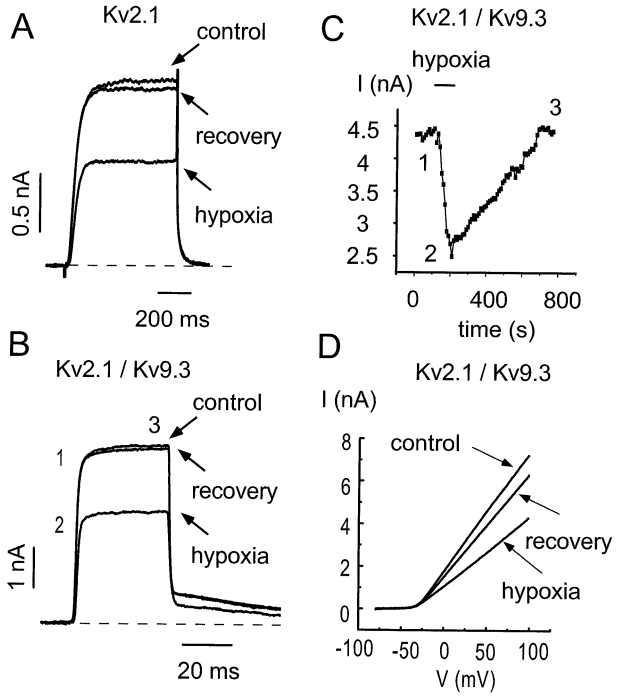

Fig. 9. Hypoxic inhibition of Kv2.1 and Kv2.1/Kv9.3 in COS cells. (**A**) Reversible inhibition of Kv2.1 by a 5-min hypoxic period. (**B**) Reversible hypoxic inhibition of Kv2.1/Kv9.3. Timing of hypoxia is indicated in panel (C) by numbers. The holding potential was –60 mV and the test pulse was +30 mV. (**C**) Time course of Kv2.1/Kv9.3 current inhibition by hypoxia. (**D**) *I–V* curves of Kv2.1/Kv9.3 showing the reversible inhibition by 5 min of hypoxia. The holding potential was –80 mV and the cell was depolarized with a voltage ramp of 350 ms in duration to 100 mV.

Hypoxic inhibition of Kv2.1 and Kv2.1/Kv9.3

It has been hypothesized that the oxygen sensor could be a structural part of the oxygen-sensitive K^+ channels (for review, see Weir and Archer, 1995). During normoxia, the channel would be in an oxidized open state and during hypoxia, the reduced form of the channel would be closed (Ruppersberg *et al.*, 1991; Duprat *et al.*, 1995). Another hypothesis suggested that the K^+ channels expressed in the oxygen-sensitive cells (PA, type I carotid body and pulmonary neuroepithelial body cells) are closely associated with a membrane-bound oxygen sensor such as an NADPH oxidase (Youngson *et al.*, 1993; Wang *et al.*, 1996). Alternatively, oxygen regulation has been proposed to be a consequence of variation in the level of intracellular metabolites such as ATP, oxyradicals, cytochrome P450 products and intracellular calcium (Archer *et al.*, 1993; Yuan *et al.*, 1994, 1995a,b, 1996; Bright *et al.*, 1995; Post *et al.*, 1995).

In the present study, we observed that in a subset of transfected COS cells, Kv2.1 and Kv2.1/Kv9.3 were reversibly inhibited by hypoxia. Since hypoxic sensitivity was not detected in all the cells tested, these results imply that the oxygen sensor is not a structural part of the Kv2.1/Kv9.3 complex, but rather an oxygen reactive structure endogenously expressed in only a subset of our COS cells.

Very recently, it has been demonstrated that the $I_{K(N)}$ current which is active at resting potential is reversibly inhibited by hypoxia and is involved in the hypoxic depolarization of rabbit PA myocytes (Osipenko *et al.*, 1997). Considering the biophysical, pharmacological and hypoxic regulation properties of $I_{K(N)}$, it is tempting to suggest that Kv2.1/Kv9.3 may encode $I_{K(N)}$ in PA smooth muscle cells.

Metabolic regulation of Kv2.1/Kv9.3 and hypoxic pulmonary artery vasoconstriction

Our finding that intracellular ATP activates, and that hypoxia inhibits Kv2.1 and Kv2.1/Kv9.3, raises the question of the role of this regulation in PA smooth muscle cells and their possible implications for hypoxic pulmonary vasoconstriction (HPV). Several arguments strongly suggest that the PA hypoxic contractile response is at least partly dependent on the glycolytic pathway. First, in the perfused rat lung, inhibitors of oxidative phosphorylation and glycolysis cause transient pressor responses and potentiate hypoxic vasoconstriction (Rounds and McMurtry, 1981). Secondly, 2-deoxyglucose and carbonyl cyanide *p*-trifluoromethoxyphenylhydrazone (FCCP) decrease the activity of voltage-dependent K^+ channels, raise intracellular Ca^{2+} and trigger contraction of isolated PA smooth muscle cells (Yuan *et al.*, 1994, 1996). Thirdly, rotenone and antimycin A which have been demonstrated to decrease the production of activated oxygen species from the electron transport chain and the synthesis of ATP, inhibit K^+ currents in PA myocytes and mimic HPV (Archer *et al.*, 1993). Fourthly, a direct effect of intracellular ATP on Kv channels in rabbit PA smooth muscle cells has been demonstrated, whereby an elevation in intracellular ATP levels induced an important increase in the delayed-rectifier K^+ current amplitude (Evans *et al.*, 1994). Taken together, these data suggest that the delayed-rectifier K^+ channels, among them Kv2.1 and Kv2.1/Kv9.3, are regulated by local metabolic conditions in PA cells and that their activities are tightly linked to internal ATP and possibly to activated oxygen species from the electron transport chain. Most importantly, given the ATP sensitivity in the millimolar range of both Kv2.1 and Kv2.1/Kv9.3 near physiological concentrations, these channel complexes must be extremely sensitive to the metabolic status of the cell.

Table I. PCR primer sets, predicted sizes and annealing temperatures

	Primer sets 5′ to 3′	Size	Temperature (°C)
Rat β actin	TTGTAACCAACTGGGACGATATGG GATCTTGATCTTCATGGTGCTAGG	764 bp	60
Kv9.3	TCCCATCACCATCATCTTCAA GCCGTAGCAATAAATCCTTCC	569 bp	50
Kv1.2	AACAGGACTAATGCAGATATT TAAGTGGGAAGATAGGTGGTG	283 bp	50
Kv1.3	TCCCTCTCCCTATTGCTTCAT CTGTTTTCGTTTCATCTGTTG	1.1 kb	55
Kv1.5	GGCGACTGCTGTTATGAGGAG ACTGGAGGTGTTGGAATGCTA	1.4 kb	55
Kv2.1	GCAGGAGAAATCAAGGAGGAG ATAAAGCCCCAGGGACCACAG	496 bp	60

Segmental expression of Kv2.1/Kv9.3 in pulmonary artery

It has been suggested that a differential distribution of voltage-dependent, delayed-rectifier K^+ channels in conduit and resistance arteries determines their response to hypoxia (Archer *et al.*, 1996). Hypoxia causes sustained constriction of resistance arteries and conversely relaxation in conduit arteries (Bennie *et al.*, 1991; Jin *et al.*, 1992) These effects have been correlated with a higher expression of oxygen-reactive, delayed-rectifier K^+ channels in resistance arteries (Archer, 1996; Archer *et al.*, 1996). By contrast the oxygen-sensitive $I_{K(N)}$ was found at all levels along the PA tree (Evans *et al.*, 1996; Osipenko *et al.*, 1997).

Kv2.1 transcript levels were higher in conduit compared with resistance arteries, while Kv9.3 was expressed at similar levels in both segments. These results suggest that differential translational and/or post-translational controls rather than transcriptional control may be involved in the segmental expression of oxygen-sensitive delayed-rectifier $I_{K(V)}$ and $I_{K(N)}$ channels.

The anorexic agent dex-fenfluramine blocks Kv2.1 and Kv2.1/Kv9.3 channels

Pulmonary hypertension is a dramatic disease which ultimately provokes right heart failure and death within 2 to 5 years. It occurs in people living at high altitude and in patients suffering from chronic obstructive lung diseases such as chronic bronchitis and emphysema (Barnes and Liu, 1995). Furthermore, it has been demonstrated that anorexic agents such as aminorex fumarate and DFF have caused an epidemic of pulmonary hypertension in Europe. Interestingly, these compounds have been recently shown to inhibit K^+ currents in rat pulmonary artery myocytes and to cause pulmonary vasoconstriction (Weir *et al.*, 1996). In the present report we confirm these data and further demonstrate that Kv2.1 and Kv2.1/Kv9.3 complexes are similarly sensitive to the hypertensive anorexic agent, DFF.

In conclusion, our results support the idea that, in PA myocytes, the Kv2.1 and Kv2.1/Kv9.3 complexes are components of the ATP-sensitive delayed-rectifier K^+ channels. The voltage activation threshold of the Kv2.1/Kv9.3 complex indicates that it may play a role in the establishment of the resting membrane potential of PA myocytes and in the control of the action potential duration. The biophysical, pharmacological and regulation profiles of Kv2.1/Kv9.3 are identical to those of the $I_{K(N)}$ channels in PA myocytes, including sensitivity to 4-AP, resistance to TEA and CTX, and inhibition by hypoxia. The understanding of the molecular nature of the K^+ channels in PA myocytes will obviously have major therapeutic significance for important human pathologies such as pulmonary hypertension. An interesting issue would be to identify openers of these novel ATP-dependent, delayed-rectifier K^+ channels. Opening of these channels would lead to repolarization of PA myocytes, closing of calcium channels, vasorelaxation of resistance arteries and thereby a decrease in arterial pressure. Moreover, the identification of these channels may help to define novel appetite-suppressant agents devoid of side effects on the pulmonary vasculature.

Materials and methods

Isolation of K^+ channel cDNAs

Degenerate primers were designed in two highly conserved regions of K^+ channels, one upstream of S1 (5′-ISARKWITWYTWYGAYMG-3′) and the other in the H5 pore domain (5′-RTAICCIACIGTISWCAT-3′). These primers were used to amplify reverse-transcribed total RNA from dissected pulmonary arteries (PA) freed of the endothelium (as described in 'Electrophysiological studies') with 40 rounds of PCR (total reaction volume 50 μl: 20 mM Tris–Cl, pH 8.4, 50 mM KCl, 2 mM $MgCl_2$, 400 μM dNTPs, 10 μM each primer, 2.5 U of Gibco-BRL Taq polymerase and 100 ng of PA cDNA). Cycling parameters were: denaturation for 5 min at 95°C, followed by 10 cycles of 95°C for 45 s, 45°C for 2 min, 72°C for 1 min and an additional 30 cycles of 95°C for 45 s, 50°C for 2 min, 72°C for 1 min. Ten μl of the PCR reaction was run on LMP (expected size between 900 and 1000 bp) and the amplified band excised and subjected to another round of PCR. Two μl of the resulting PCR reaction was cloned into the TA cloning vector (Invitrogen). The partial cDNAs obtained in this manner were subsequently sequenced (automatic sequencer, Applied Biosystems) and used in a BLAST search, leading to the identification of Kv1.2, Kv1.3, Kv2.1 and a novel gene Kv9.3 which was used to screen 10^6 clones of a λZAP rat brain cDNA library (Stratagene) at high stringency (50% formamide, 5× SSC, 4× Denhardt, 1% SDS, 100 μg/ml herring sperm DNA, 55°C). Two independent clones were obtained which did not correspond to the full-length cDNA and lacked the 5′ end. The 5′ end was obtained from a rat kidney Lambda Fix II genomic library (Stratagene) and confirmed by RT–PCR.

Northern blot analysis

Total RNA was extracted from rat tissues following Chomcyzynski and Sacchi's procedure. Northern blot analysis was performed using 15 μg of total RNA. The probe used corresponded to the initial degenerate PCR fragment of 930 bp and was labelled using the random prime kit, Prime-It (Stratagene) and [α-^{32}P]dCTP. Hybridization was carried out at high stringency (same conditions as for the library).

RT–PCR

One μg of total RNA was reverse-transcribed using 250 ng of random primers and SUPERSCRIPT II reverse transcriptase according to the manufacturer's protocol (Gibco-BRL). PCR was performed in a volume of 25 μl in the presence of 1.5 μCi of [α-^{32}P]dCTP, 1.5 mM $MgCl_2$, 20 mM Tris–Cl, pH 8.4, 50 mM KCl, 100 ng of each primer, 200 μM dNTPs and 50 ng of template. Cycling parameters: 95°C for 5 min, followed by 35 cycles of 94°C for 45 s, X°C for 45 s (where X is the annealing temperature), 72°C for 1 min. Two μl of each reaction was resolved on a 5% polyacrylamide gel. The gel was dried and exposed to film. PCR primer sets, predicted sizes and annealing temperatures are as listed in Table I.

Metabolic labelling with [^{35}S]methionine and immunoprecipitation

Xenopus oocyte nuclei were injected with either 100 pg pCI (Promega), 100 pg pCI–Kv9.3, 100 pg pCI–Kv2.1 or 100 pg of pCI–Kv9.3 and 100 pg of pCI–Kv2.1 (final DNA concentrations were adjusted with pCI empty expression vector), incubated for 4 h in ND96, and then in ND96 containing 50 μCi/ml [^{35}S]methionine for 2–3 days at 22°C. Eight oocytes were homogenized in 300 μl of solubilization buffer (20 mM Tris–Cl, pH 7.4, 5 mM EDTA, 5 mM EGTA, 100 mM NaCl, 50 μg/ml PMSF, 1 mM iodoacetamide, 1 μM pepstatin) and centrifuged at 1000 *g* for 10 min at 4°C. Triton X-100 was added to the supernatant to a final concentration of 4% and the homogenates were spun as before. The supernatant was diluted to 1 ml with solubilization buffer and then incubated with a 1:200 dilution of anti-Kv2.1 (Upstate biotechnology) for 16 h at 4°C. The antibody–antigen complex was incubated for 1 h with protein A–Sepharose (Pharmacia) and then pelleted by brief centrifugation. Immunoprecipitates were washed four times with solubilization buffer, once with PBS and then resuspended in 50 μl of SDS sample buffer. The samples were resolved (without boiling) on a 7.5% polyacrylamide–SDS gel, with molecular weight standards, the gel dried down and exposed to film.

Oocyte injections and COS transfections

100 pg of pCI–Kv2.1 and 200 pg pCI–Kv9.3 were routinely injected (10 nl) into *Xenopus* oocyte nuclei. COS-M6 cells were transfected with 1 μg of pCI–Kv2.1, 2 μg of pCI–Kv9.3 and 1 μg of pCI–CD8 (as a marker of transfection) using the standard DEAE–dextran procedure. Final DNA concentrations were always adjusted with pCI empty expression vector.

Electrophysiological studies

Conduit (main right and left PA with an external diameter of 500–600 μm) and resistance (fourth and fifth divisions with a diameter <300 μm) pulmonary arteries were dissected in aseptic conditions from 1-month-old Sprague-Dawley rats. The pulmonary branches were cleaned, under a dissecting microscope, of all visible parenchyma and connective tissues. The endothelium was removed mechanically by threading the vessels onto a lightly sanded surgical steel rod and rotating the vessel four times in each direction. Cell isolation procedures are identical to those of Guibert *et al.* (1996). PA myocytes were cultured in H21 medium supplemented with 15% fetal bovine serum. Cells were passaged every week. Electrophysiological procedures (oocyte two microelectrode voltage clamp, COS whole cell and single channel patch clamp) have been previously described elsewhere (Honoré *et al.*, 1992).

For COS whole-cell experiments, we used an external medium of the following composition: Na^+ gluconate, 170 mM; KCl, 5 mM; $CaCl_2$, 1 mM; $MgCl_2$, 3 mM; HEPES, 10 mM; pH 7.4 with NaOH. The internal media was: K^+ gluconate, 150 mM; $MgCl_2$, 3 mM; EGTA, 10 mM; HEPES, 10 mM; Na_2ATP, 5 mM; pH 7.2 with KOH. For cell-attached single-channel studies, cells were bathed with a K^+-rich solution of the following composition: K^+ gluconate, 150 mM; $MgCl_2$, 3 mM; EGTA, 10 mM; HEPES, 10 mM; pH 7.2 with KOH and the pipette contained the external solution used for whole-cell experiments. For pulmonary artery myocyte electrophysiology, we used an external medium of the following composition: NaCl, 141 mM; KCl, 4.7 mM; $MgCl_2$, 3 mM; HEPES, 10 mM; EGTA, 5 mM; glucose, 10 mM; pH 7.4 with NaOH. The internal solution contained: KCl, 125 mM; $MgCl_2$, 4 mM; HEPES, 10 mM; EGTA, 10 mM; Na_2ATP, 5 mM, pH 7.2 with KOH. For oocyte experiments we used ND96 saline solution. The effects of hypoxia were studied by switching between normoxic and hypoxic perfusate reservoirs. The hypoxic perfusate reservoir was bubbled at least 20 min before the beginning of perfusion with 100% N_2. These procedures produced pO_2s of 160 mmHg in normoxia and 35 mmHg in hypoxia in the recording chamber. The pH and temperature were maintained at 7.4 and 25°C respectively, throughout the experiments. Rate of solution exchange was <10 s. Alkaline phosphatase, ATPγs, AMP–PNP and ADP were obtained from Sigma. CTX, DTX and MCD peptide were purified in our laboratory. Dex-fenfluramine was a gift from Servier (Paris). Dex-fenfluramine was dissolved daily as a stock solution in saline solution at a concentration of 10 mM.

Acknowledgements

We are grateful to Dr F.Lesage for his advice during the progress of this work and to all the members of our laboratory for fruitful discussion. We thank D.Doume for her secretarial assistance. This work was funded by the Centre National de la Recherche Scientifique (CNRS), the Philippe Foundation and by the Marie Curie EEC programme.

References

Archer,S.L. (1996) Diversity of phenotype and function of vascular smooth muscle cells. *J. Lab. Clin. Med.*, **127**, 524–529.

Archer,S.L., Huang,J., Henry,T., Peterson,D. and Weir,E.K. (1993) A redox-based O_2 sensor in rat pulmonary vasculature. *Circ. Res.*, **73**, 1100–1112.

Archer,S.L., Huang,J.M., Reeve,H.L., Hampl,V., Tolarova,S., Michelakis,E. and Weir,E.K. (1996) Differential distribution of electrophysiologically distinct myocytes in conduit and resistance arteries determines their response to nitric oxide and hypoxia. *Circ. Res.*, **78**, 431–442.

Barnes,P.J. and Liu,S.F. (1995) Regulation of pulmonary vascular tone. *Pharmacol. Rev.*, **47**, 87–131.

Baumann,A., Grupe,A., Ackermann,A. and Pongs,O. (1988) Structure of the voltage-dependent potassium channel is highly conserved from *Drosophila* to vertebrate central nervous systems. *EMBO J.*, **7**, 2457–2463.

Beckh,S. and Pongs,O. (1990) Members of the RCK potassium channel family are differentially expressed in the rat nervous system. *EMBO J.*, **9**, 777–782.

Bennie,R.E., Packer,C.S., Powell,D.R., Jin,N. and Rhoades,R.A. (1991) Biphasic contractile response of pulmonary artery to hypoxia. *Am. J. Physiol.*, **261**, L156–L163.

Bright,R.T., Salvaterra,C.G., Rubin,L.J. and Yuan,X.J. (1995) Inhibition of glycolysis by 2-DG increases $[Ca^{2+}]_i$ in pulmonary arterial smooth muscle cells. *Am. J. Physiol.*, **269**, L203–L208.

Cornfield,D.N., Stevens,T., McMurtry,I.F., Abman,S.H. and Rodman,D.M. (1994) Acute hypoxia causes membrane depolarization and calcium influx in fetal pulmonary artery smooth muscle cells. *Am. J. Physiol.*, **266**, L469–L475.

Drewe,J.A., Verma,S., Frech,G. and Joho,R.H. (1992) Distinct spatial and temporal expression patterns of K^+ channel mRNAs from different subfamilies. *J. Neurosci.*, **12**, 538–548.

Duprat,F., Guillemare,E., Romey,G., Fink,M., Lesage,F., Lazdunski,M. and Honoré,E. (1995) Susceptibility of cloned K^+ channels to reactive oxygen species. *Proc. Natl Acad. Sci. USA*, **92**, 11796–11800.

Evans,A.M., Clapp,L.H. and Gurney,A.M. (1994) Augmentation by intracellular ATP of the delayed rectifier current independently of the glibenclamide-sensitive K-current in rabbit arterial myocytes. *Br. J. Pharmacol.*, **111**, 972–974.

Evans,A.M., Osipenko,O.N. and Gurney,A.M. (1996) Properties of a novel K^+ current that is active at resting potential in rabbit pulmonary artery smooth muscle cells. *J. Physiol.*, **496**, 407–420.

Frech,G.C., VanDongen,A.M., Schuster,G., Brown,A.M. and Joho,R.H. (1989) A novel potassium channel with delayed rectifier properties isolated from rat brain by expression cloning. *Nature*, **340**, 642–645.

Guibert,C., Pacaud,P., Loirand,G., Marthan,R. and Savineau,J.P. (1996) Effect of extracellular ATP on cytosolic Ca^{2+} concentration in rat pulmonary artery myocytes. *Am. J. Physiol.*, **271**, L450–L458.

Honoré,E., Attali,B., Romey,G., Lesage,F., Barhanin,J. and Lazdunski,M. (1992) Different types of K^+ channel current are generated by different levels of a single mRNA. *EMBO J.*, **11**, 2465–2471.

Hugnot,J.P., Salinas,M., Lesage,F., Guillemare,E., de Weille,J., Heurteaux,C., Mattei,M.G. and Lazdunski,M. (1996) Kv8.1, a new neuronal potassium channel subunit with specific inhibitory properties towards *Shab* and *Shaw* channels. *EMBO J.*, **15**, 3322–3331.

Jin,N., Packer,C.S. and Rhoades,R.A. (1992) Pulmonary arterial hypoxic contraction: signal transduction. *Am. J. Physiol.*, **263**, L73–L78.

Kozlowski,R.Z. (1995) Ion channels, oxygen sensation and signal transduction in pulmonary arterial smooth muscle. *Cardiovasc. Res.*, **30**, 318–325.

Lopez-Barneo,J. (1994) Oxygen-sensitive ion channels: how ubiquitous are they? *Trends Neurosci.*, **17**, 133–135.

Lopez-Barneo,J. (1996) Oxygen-sensing by ion channels and the regulation of cellular functions. *Trends Neurosci.*, **19**, 435–440.

Lopez-Barneo,J., Ortega-Saenz,P., Molina,A., Franco-Obregon,A., Urena,J. and Castellano,A. (1997) Oxygen sensing by ion channels. *Kidney Int.*, **51**, 454–461.

Osipenko,O.N., Evans,A.M. and Gurney,A.M. (1997) Regulation of the resting potential of rabbit pulmonary artery myocytes by a low threshold, O_2-sensing potassium current. *Br. J. Pharmacol.*, **120**, 1461–1470.

Pongs,O. (1992) Molecular biology of voltage-dependent potassium channels. *Physiol. Rev.*, **72**, S69–S88.

Post,J.M., Hume,J.R., Archer,S.L. and Weir,E.K. (1992) Direct role for potassium channel inhibition in hypoxic pulmonary vasoconstriction. *Am. J. Physiol.*, **262**, C882–C890.

Post,J.M., Gelband,C.H. and Hume,J.R. (1995) $[Ca^{2+}]_i$ inhibition of K^+ channels in canine pulmonary artery. Novel mechanism for hypoxia-induced membrane depolarization. *Circ. Res.*, **77**, 131–139.

Post,M.A., Kirsch,G.E. and Brown,A.M. (1996) Kv2.1 and electrically silent Kv6.1 potassium channel subunits combine and express a novel current. *FEBS Lett.*, **399**, 177–182.

Quast,U. and Cook,N.S. (1989) Moving together: K^+ channel openers and ATP-sensitive K^+ channels. *Trends Pharmacol. Sci.*, **10**, 431–434.

Rounds,S. and McMurtry,I.F. (1981) Inhibitors of oxidative ATP production cause transient vasoconstriction and block subsequent pressor responses in rat lungs. *Circ. Res.*, **48**, 393–400.

Ruppersberg,J.P., Stocker,M., Pongs,O., Heinemann,S.H., Frank,R. and Koenen,M. (1991) Regulation of fast inactivation of cloned mammalian IK(A) channels by cysteine oxidation. *Nature*, **352**, 711–714.

Salinas,M., de Weille,J., Guillemare,E., Lazdunski,M. and Hugnot,J.P. (1997a) Modes of regulation of shab K^+ channel activity by the Kv8.1 subunit. *J. Biol. Chem.*, **272**, 8774–8780.

Salinas,M., Duprat,F., Heurteaux,C., Hugnot,J.P. and Lazdunski,M. (1997b) New modulatory α subunits for mammalian *Shab* K^+ channels. *J. Biol. Chem.*, **272**, 24371–24379.

Shi,G., Kleinklaus,A.K., Marrion,N.V. and Trimmer,J.S. (1994) Properties of Kv2.1 K^+ channels expressed in transfected mammalian cells. *J. Biol. Chem.*, **269**, 23204–23211.

Smirnov,S.V., Robertson,T.P., Ward,J.P. and Aaronson,P.I. (1994) Chronic hypoxia is associated with reduced delayed rectifier K^+ current in rat pulmonary artery muscle cells. *Am. J. Physiol.*, **266**, H365–H370.

Stuhmer,W., Ruppersberg,J.P., Schroter,K.H., Sakmann,B., Stocker,M., Giese,K.P., Perschke,A., Baumann,A. and Pongs,O. (1989) Molecular basis of functional diversity of voltage-gated potassium channels in mammalian brain. *EMBO J.*, **8**, 3235–3244.

Wang,D., Youngson,C., Wong,V., Yeger,H., Dinauer,M.C., Vega-Saenz Miera,E., Rudy,B. and Cutz,E. (1996) NADPH-oxidase and a hydrogen peroxide-sensitive K^+ channel may function as an oxygen sensor complex in airway chemoreceptors and small cell lung carcinoma cell lines. *Proc. Natl Acad. Sci. USA*, **93**, 13182–13187.

Weir,E.K. and Archer,S.L. (1995) The mechanism of acute hypoxic pulmonary vasoconstriction: the tale of two channels. *FASEB J.*, **9**, 183–189.

Weir,E.K., Reeve,H.L., Huang,J.M., Michelakis,E., Nelson,D.P., Hampl,V. and Archer,S.L. (1996) Anorexic agents aminorex, fenfluramine, and dexfenfluramine inhibit potassium current in rat pulmonary vascular smooth muscle and cause pulmonary vasoconstriction. *Circulation*, **94**, 2216–2220.

Youngson,C., Nurse,C., Yeger,H. and Cutz,E. (1993) Oxygen sensing in airway chemoreceptors. *Nature*, **365**, 153–155.

Yuan,X.J. (1995) Voltage-gated K^+ currents regulate resting membrane potential and $[Ca^{2+}]_i$ in pulmonary arterial myocytes. *Circ. Res.*, **77**, 370–378.

Yuan,X.J., Goldman,W.F., Tod,M.L., Rubin,L.J. and Blaustein,M.P. (1993a) Hypoxia reduces potassium currents in cultured rat pulmonary but not mesenteric arterial myocytes. *Am. J. Physiol.*, **264**, L116–L123.

Yuan,X.J., Goldman,W.F., Tod,M.L., Rubin,L.J. and Blaustein,M.P. (1993b) Ionic currents in rat pulmonary and mesenteric arterial myocytes in primary culture and subculture. *Am. J. Physiol.*, **264**, L107–L115.

Yuan,X.J., Tod,M.L., Rubin,L.J. and Blaustein,M.P. (1994) Deoxyglucose and reduced glutathione mimic effects of hypoxia on K^+ and Ca^{2+} conductances in pulmonary artery cells. *Am. J. Physiol.*, **267**, L52–L63.

Yuan,X.J., Tod,M.L., Rubin,L.J. and Blaustein,M.P. (1995a) Hypoxic and metabolic regulation of voltage-gated K^+ channels in rat pulmonary artery smooth muscle cells. *Exp. Physiol.*, **80**, 803–813.

Yuan,X.J., Tod,M.L., Rubin,L.J. and Blaustein,M.P. (1995b) Inhibition of cytochrome P-450 reduces voltage-gated K^+ currents in pulmonary arterial myocytes. *Am. J. Physiol.*, **268**, C259–C270.

Yuan,X.J., Sugiyama,T., Goldman,W.F., Rubin,L.J. and Blaustein,M.P. (1996) A mitochondrial uncoupler increases KCa currents but decreases KV currents in pulmonary artery myocytes. *Am. J. Physiol.*, **270**, C321–C331.

Received on July 8, 1997; revised on August 15, 1997